34th Annual International Conference of the IEEE EMBS
San Diego, California USA, 28 August - 1 September, 2012

Numerical Simulation of Single-Cell Electroporation with an Electrolyte Filled Capillary Experimental Set-up

Rafael A. Chiea[1], Daniela O. H. Suzuki[2] and Jefferson L.B. Marques[3]

Abstract— **Electroporation experiments can be divided in bulk type and single-cell type (SCEP). In bulk electroporation, homogeneous electric field is applied to a cell suspension. An example of SCEP is electrolyte-filled capillary (EFC) experiments, where an inhomogeneous field is focused on a single-cell. In this work, results of numerical simulation of electroporation for an EFC experiment geometry are presented. Better spacial resolution in comparison with bulk electroporation was observed. Rapid creation of a great number ($\sim 10^5$) of pores leads to pore radius around 100 times smaller than when pores are created slowly and in lower quantity (~ 10). The model could be used to understand how stimulus waveform influences pore count and size, which may help to better control electroporation in SCEP experiments using EFC.**

I. INTRODUCTION

When cell membrane is exposed to sufficiently high electric field, transmembrane potential increases and nanoscale pores are formed in the cell membrane, increasing its permeability. This phenomenon is termed electroporation[1]. From a experimental point-of-view, electroporation devides into two main groups: bulk and single-cell electroporation (SCEP). Unlike bulk electroporation, in which a homogeneous electric field is applied to a cell suspension ,in SCEP, either the studied cell is isolated from its population, either an inhomogeneous electric field is focused on the target cell. SCEP allows the study of a single cell of specific size, shape and status, while in bulk electroporation there is a wide distribution of outcomes among cells in suspension[2].

One way to focus the electric field on the target cell is to use an electrolytic filled capillary (EFC)[3][4][5]. The experimental set-up geometry can be seen on figure 1. An EFC is placed at a distance d, a few micrometers from the cell membrane. A high electric potential, of the order of hundreds to thousands of Volts, is then applied to the EFC, and an inhomogeneous electric field appears between the tip of the capillary and a reference electrode in the solution. One major advantage of EFC experiments is the possibility to use patch-clamp whole-cell recording method to obtain transient pore information[2].

*This work was financially supported by CNPq - Brazil.

[1]R. A. Chiea is with the Institute of Biomedical Engineering (IEB-UFSC), Federal University of Santa Catarina. UFSC - CTC - Departament of Eletrical Engineering +55 48 37218686, 88040-900, Florianopolis, SC -Brazil. rafael.chiea ieb.ufsc.br

[2]D. Suzuki is with the Institute of Biomedical Engineering (IEB-UFSC), Federal University of Santa Catarina. UFSC - CTC - Departament of Eletrical Engineering +55 48 37218686, 88040-900, Florianopolis, SC -Brazil. suzuki eel.ufsc.br

[3]J.L.B. Marques is with the Institute of Biomedical Engineering (IEB-UFSC), Federal University of Santa Catarina. UFSC - CTC - Departament of Eletrical Engineering +55 48 37218686, 88040-900, Florianopolis, SC -Brazil. jmarques ieb.ufsc.br

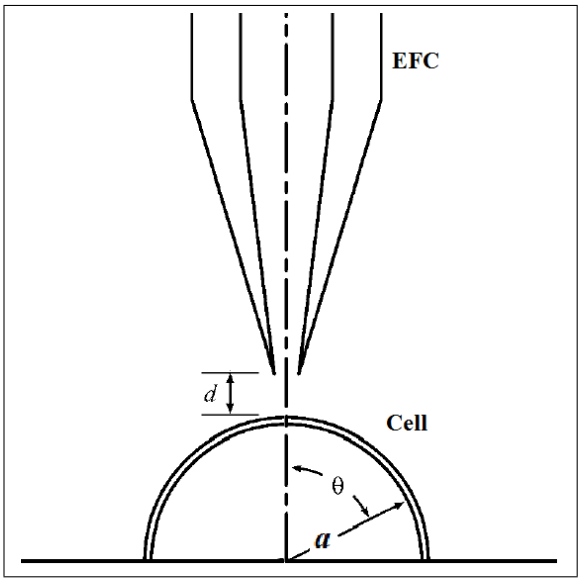

Fig. 1. Experimental set-up geometry for EFC single-cell electroporation

Numerical simulations of SCEP have been reported in the last decade[6][7][8]. Even though these works refer to single-cell electroporation, they consider a homogeneous electric field applied to the cell, which is more appropriated to a bulk electroporation set-up. Zudans[9] have calculated the induced transmembrane potential for an EFC experimental set-up, using finite element method. However, studies of pore creation and evolution on cells subjected to inhomogeneous fields have not yet been reported.

Understanding how inhomogeneous electrical field applied by an EFC affects membrane pore creation and pore radii evolution might help to develop techniques to control cell electroporation in experiments based in this set-up. In this paper, first results of numerical simulation of SCEP on an inhomogeneous electric field are presented.

II. MODEL

According to electroporation theory[10][11], all pores are initialy hydrophobic and most of them are quickly destroyed by lipid fluctuation. However, if pores with radius bigger than $r > r^*$ are created, they spontaneously become hydrophilic pores, interest of this study, which have a longer life. The hydrophilic pores creation rate is given by[12]

$$\frac{\mathrm{d}N}{\mathrm{d}t} = \alpha e^{(V_m/V_{ep})^2}\left(1 - \frac{N}{N_{eq}(V_m)}\right) \quad (1)$$

where N is the density of pores, α is the pore creation rate coefficient, V_m is the transmembrane potential and Vep is the characteristic voltage of electroporation. N_eq is the equilibrium density of pores for a given V_m, and is given by the following equation.

$$N_{eq} = N_0 e^{q\left(V_m/V_{ep}\right)^2} \tag{2}$$

N_0 is the equilibrium density of pores for $V_m = 0$ and $q = (r_m/r^*)^2$.

As hydrophilic pores are created, they immediately expand to the minimum energy radius, r_m. Therefore, in this study it is considered that pores are created with initial radius r_m. Pores radii then change in order to minimize the energy of the entire lipid bilayer, W. Size changes of each pore j of a total of n pores, $j = 1,2,\ldots,n$, is determined by[6]

$$\frac{\mathrm{d}r_j}{\mathrm{d}t} = -\frac{D_p}{k_B T}\frac{\partial W}{\partial r_j} \qquad j = 1,2,\cdots,n. \tag{3}$$

where D_p is the diffusion coefficient for pore radius, k_B is the Boltzmann constant and T is the temperature.

The bilayer energy W is given by

$$W = \sum_{j=1}^{n}\left\{\beta\left(\frac{r_0}{r_j}\right)^4 + 2\pi^2 r_j \kappa\left(\frac{1}{h} - \psi c_0\right) - \pi\sigma_{eff}A_p r_j^2 + \int_0^{r_j} F(r_j, V_m)\,\mathrm{d}r\right\} \tag{4}$$

Equation 4 indicates that W is composed of four terms. The first term accounts for steric repulsion of lipids heads, where β is an energy constant. The second term represents the edge energy of the pore perimeter, considering the presence of cholesterol[7], where κ is the bending modulus of the membrane, h is the membrane thickness, ψ is the mole fraction of cholesterol in the membrane and c_0 is the spontaneous curvature for cholesterol.

The third term refers to the effect of pores in the membrane tension. σ_{eff} is a function of the total area of the pores, $A_p = \sum_{j=1}^{n}\pi r_j^2$.

$$\sigma_{eff} = 2\sigma' - \frac{\sigma' - \sigma_0}{(1 - \frac{A_p}{A_t})^2} \tag{5}$$

The contribution of transmembrane voltage is represented in the last term by the electric force F, which is given by

$$F = \frac{F_{max}}{1 + \frac{r_h}{r_j + r_t}} \cdot V_m^2 \tag{6}$$

where F_max, r_h and r_t are constants.

The evolution of the transmembrane potential on time is obtained using the following equation[1]

$$\frac{\mathrm{d}V_m}{\mathrm{d}t} + \frac{G_m + \frac{C_m}{\tau_0}}{C_m + C_w}V_m = -\frac{V_0}{\tau_0 + \frac{\varepsilon_w}{\sigma_i}} \tag{7}$$

$$Gm = \sum_{j=1}^{n}\left(\frac{h}{s_o \pi r_j^2} + \frac{1}{2 s_o r_j}\right)^{-1} \tag{8}$$

$$C_w = \frac{\varepsilon_w}{a\left(1 + \frac{s_i}{2 s_o}\right)} \tag{9}$$

$$\tau_0 = a C_m (s_i + 2 s_o)^{-1} \tag{10}$$

Parameters values and definitions are indicated on table I.

TABLE I

PARAMETERS VALUES AND DESCRIPTION

Symbol	Value	Definition
a	$10\ \mu m$	Cell radius
r^*	$0.51\ nm$	Minimal radius of hydrophilic pores [8]
r_m	$0.8\ nm$	Minimum energy radius [8]
V_ep	$258\ mV$	Characteristic voltage of electroporation [8]
α	$10^9\ m^{-2}s^{-1}$	Creation rate coefficient [8]
D_p	$5\times10^{-14}\ m^2/s$	Difusion coefficient for pore radius [8]
k_B	$1.38\times10^{-23}\ J/K$	Boltzmann constant
T	$310\ K$	Temperature
β	$1.4\times10^{-19}\ J$	Steric repulsion energy [8]
h	$7\ nm$	Membrane thickness
c_0	$0.9\times10^9\ m^{-1}$	Sponteneous curvature for cholesterol [7]
κ	2.7×10^{-20}	Bending modulus of the membrane [7]
ψ	0.2	Mole fraction of cholesterol in the membrane [7]
σ	$2\times10^{-2}\ J/m^2$	Tension of hydrocarbon-water interface [8]
σ_0	$10^{-6}\ J/m^2$	Tension of bilayer without pores [8]
F_{max}	$7.0\times10^{-10}\ N/V^2$	Maximum electric force $@V_m = 1V$ [8]
r_h	$0.97\ nm$	Constant in (6) for avection velocity [8]
r_t	$0.31\ nm$	Constant in (6) for avection velocity [8]
C_m	$10^{-2}\ Fm^{-2}$	Membrane capacitance [8]
N_0	$1.5\times10^9\ m^{-2}$	Equilibrium density of pores $@V_m = 0V$ [8]
s_i	$0.6\ Sm^{-1}$	Cytoplasm conductance[13]
s_o	$0.23\ Sm^{-1}$	External solution conductance[13]
ε_w	80	Water permittivity
d	$4\ \mu m$	Distance between EFC tip and cell membrane

III. METHODS

A computer program using C++ language was developed for dynamic simulation of single-cell electroporation. The results of Zudans[9] for the transmembrane voltage in regime were used as input for the program. Numerical integration of (1), (3) and (7) was performed using the Runge-Kutta 4th order method.

Spherical geometry is used to represent the cell because of its mathematical simplicity and also in order to compare our results with reported ones[7][8]. In EFC experiments with adherent cells, the cell is represented as a half-sphere on a surface (Figure 1). This half-sphere was divided in 90 ring segments, at each 1° of θ. The transmembrane voltage V_m, the number of pores n, the average radius r_{avg} and the maximum radius r_{max} were calculated for each segment. At

initial time instant ($t = 0$), cell is considered to be resting, so all variables calculated are considered to value zero.

IV. RESULTS AND DISCUSSION

Numeric simulation of SCEP was performed for a voltage pulse $2\,kV$ and $1\,ms$ of duration applied to the EFC. The results are shown fig. 2. To analyse the results, four regions were defined in the cell membrane: region I, $|\theta| <= 10°$; region II, $10° < |\theta| <= 15°$; region III, $15° < |\theta| <= 20°$; and region IV, $20° < |\theta| <= 90°$. Regions are also indicated on fig. 2.

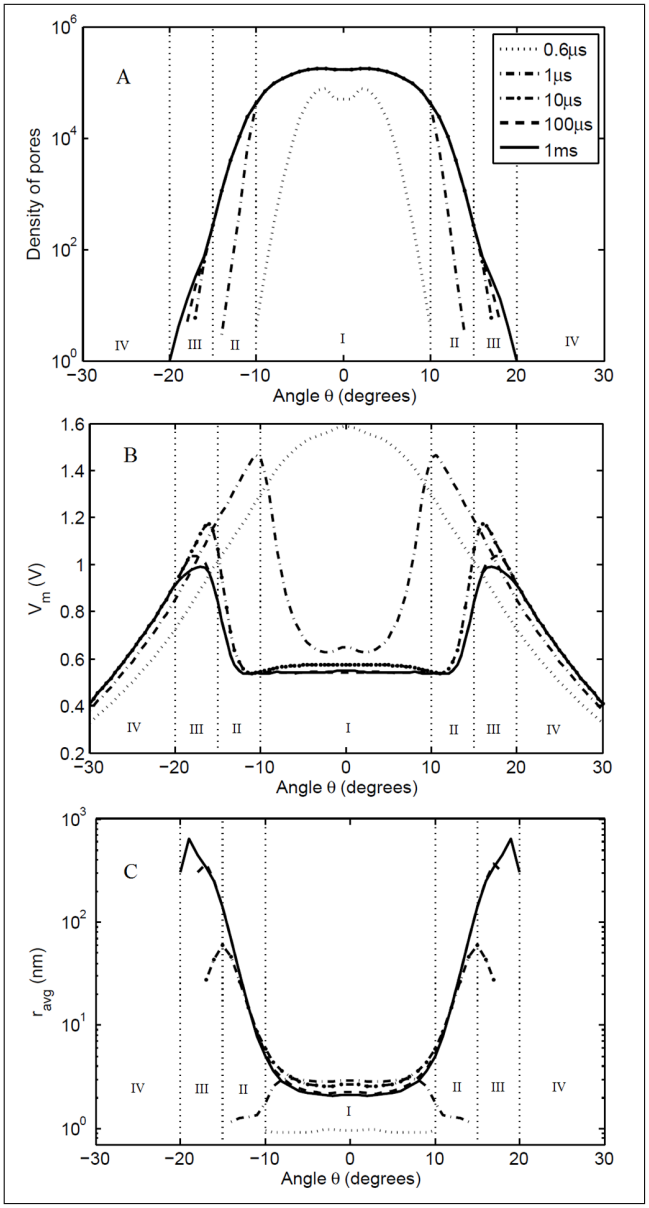

Fig. 2. Spacial distribution of the results of numerical simulation for applied tension $V = 2\,kV$ during $1\,ms$. On A density of pores, B - Transmembrane voltage and C - Average radius. For $|\theta| > 20°$, transmembrane potential is not sufficient for the creation of pores within $1\,ms$.

Fig. 2 A shows density of pores distribution on cell surface for different instants of time. A great number of pores is created in region I (density of pores$\sim 10^5$), in less than $1\,\mu s$. This is due to the quick increase of transmembrane potential up to $1.5V$, as shown by the dotted line ($0.6\,\mu s$) in fig. 2 B. This rapid augmentation of the number of pores, increases membrane conductance G_m, and consequently V_m quickly diminishes, as seen in the other curves of fig. 2 B. Following V_m, pore radius in region I increases to a maximum around $3\,nm$ and then stabilizes over $2nm$ (fig. 2 C). Maximum radius stabilizes at $10\,nm$.

In region III, $15° < |\theta| <= 20°$, pores are created slowly and in lower quantities, from the unity to a few hundreds during all simulation time. Membrane conductivity increases at a slower rate due to the lower quantity of pores. Transmembrane voltage reaches rapidly its maximum and decreases slowly. It can be seen in fig. 2B. For this region, at $1\,\mu s$ transmembrane voltage of about $1.1\,V$ is almost achieved and by the end of simulation, at $1\,ms$ this voltage is slightly lower, $0.98V$. This way, pores are created and their radii grow up to hundreds of nm, until V_m sufficiently drops to stabilize pore radii. Some radii of region III do not completely stabilize until the end of simulation time, $1\,ms$, although they show a tendency to do so in a few hundreds of nm.

Region II can be seen as an intermediary between regions I and III. As θ increases, the density of pores diminishes and pore radii is greater. The model predicts no pore creation in region IV during all simulation time. Transmembrane voltage induced by the external field in this region is not sufficient to trigger pore creation within $1\,ms$. Spacial resolution is enhanced in EFC experiments in comparison with homogeneous field set-up, were pores are creation is observed in the space of $|\theta| < 45°$[7][8].

Quick formation of a high quantity of pores leads to small pores, and slow creation of few pores leads to big pores. This behaviour is in accordance with the results of Krassowska[8]. Pore creation and size depend on transmembrane voltage, that could be regulated by the applied electric field, independently of the experimental set-up. Simulations were performed considering the applied field as a pulse, and the relations between field intensity and pore dynamics are not obvious. Varying the electric field after pore creation may be an option to control the number of pores and their size. Studying how these field variations would influence the behaviour of the pores may help to develop protocols to optimize the effect according to the application.

EFC experiments using lower voltages and longer pulses than the simulated in this work have been reported. Trains of pulse have also been used and may be better studied. Olofsson *et al.* applied a train of 30 pulses of amplitude 180 to 250 V with duration of 1 to 10 ms with 100 ms intervals[5]. Agarwal *et al.* used 500 V pulses with 500 ms of duration[4]. According to the results obtained here, these pulse characteristics may lead to few pore creation and great pore radii. Simulation must be performed to confirm this hypothesis and verify if the model outcomes fit experimental results.

V. CONCLUSION

First results of numeric simulation of pore creation and evolution in electroporation experiments using EFC are presented in this work. Information about the relations between applied field, induced transmembrane voltage, number of created pores and pore size evolution was gathered. Future work include simulation of other cell geometries and pulse configurations, experimentation and validation of the model.

Reported EFC electroporation uses less intense and longer duration pulses. Pore behaviour may be verified through numeric simulation for these conditions. Simulations may also be performed to study the influence of the waveforms of the applied field on pore evolution. Experiments may be performed in order to verify and validate the model. Since transient pore information can be obtained through patch-clamp recording during EFC experiment, numeric simulation results may be compared with experimental data.

REFERENCES

[1] D.O.H. Suzuki, A. Ramos, M.C.M. Ribeiro, L.H. Cazarolli, F.R.M.B. Silva, L.D. Leite, and J.B. Marques, Theoretical and Experimental Analisys of Electroporated Membrane Conductance en Cell Suspension. IEEE Transactions on Biomedical Engineering, vol. 58, pp. 3310-3318, 2011.

[2] M. Wang, O. Owar, J. Olofsson and S.G, Weber, Single-cell electroporation. *Anal. Bioanal. Chem.* vol. 397, pp. 3235-3248, 2010

[3] K. Nolkrantz, C. Farre, A. Brederlau, R.I.D. Karlsson, C. Brennan, P.S. Eriksson, S.G. Weber, M. Sandberg, and O. Orwar, Electroporation of Single Cells and Tissues with an Electrolyte-filled Capillary. *Anal. Chem.*, vol. 73, pp. 4469-4477, 2001.

[4] A. Agarwal, I. Zudans, E.A. Weber, J. Olofsson, O. Orwar and S. G. Weber, Effect of Cell Size and Shape on Single-Cell Electroporation, Anal. Chem., vol. 79, pp. 3589-3596, 2007.

[5] J. Olofsson, M. Levin, A. Stro1mberg, S.G. Weber, F. Ryttson and O. Orwar, Scanning Electroporation of Selected Areas of Adherent Cell Cultures, Anal. Chem., vol. 79, pp. 4410-4418, 2007.

[6] K.C. Smith, J.C. Neu and W. Krassowska, Model of Creation and Evolution of Stable Electropores for DNA Delivery, Biophys. J., vol.86, pp.2813-2826, May 2004.

[7] P. Shil1, S. Bidaye and P.B. Vidyasagar, Analysing the effects of surface distribution of pores in cell electroporation for a cell membrane containing cholesterol, J. Phys. D: Appl. Phys., vol. 41, 2008.

[8] W. Krassowska and P. D. Filev, Modeling electroporation in a single cell, Biophys. J., vol. 92, pp. 404?417, Jan. 2007.

[9] I. Zudans, A. Agarwal, O. Orwar and S. G. Weber, Numerical Calculations of Single-Cell Electroporation with an Electrolyte-Filled Capillary. Biophysical Journal, vol. 92, pp. 3696?3705, May 2007.

[10] J. C. Weaver and Y. A. Chizmadzhev, Theory of electroporation: A review, Bioelectrochemistry, vol. 41, pp. 135?160, Dec. 1996.

[11] C. Chen *et al.* Membrane electroporation theories: a review, Med. Biol. Eng. Comput., vol. 44, pp. 5-14, 2006.

[12] J.C. Neu and W. Krassowska, Asymptotic model of electroporation, Phys. Review E, vol. 59, n. 3, pp.3471-3482, Mar 1999.

[13] T. Kotnik, F. Bobanovic and D. Miklavcic, Sensitivity of transmembrane voltage induced by applied electric fields - A theoretical analysis, Bioelectrochemistry and Bioenergetics, vol. 43, pp. 285-291, 1997.